

---

# DIRECTED DIFFUSION: DIRECT CONTROL OF OBJECT PLACEMENT THROUGH ATTENTION GUIDANCE

---

A PREPRINT

**Wan-Duo Kurt Ma**  
Victoria University of Wellington  
mawand@ecs.vuw.ac.nz

**J.P. Lewis**  
Google Research  
noisebrain@gmail.com

**Avishek Lahiri**  
Google Research

**Thomas Leung**  
Google Research

**W. Bastiaan Kleijn**  
Victoria University of Wellington and Google  
bastiaan.kleijn@vuw.ac.nz

July 12, 2023

**Keywords** denoising diffusion · text-to-image generative models · artist guidance · storytelling

## ABSTRACT

Text-guided diffusion models such as DALL·E 2, Imagen, and Stable Diffusion are able to generate an effectively endless variety of images given only a short text prompt describing the desired image content. In many cases the images are of very high quality. However, these models often struggle to compose scenes containing several key objects such as characters in specified positional relationships. The missing capability to “direct” the placement of characters and objects both within and across images is crucial in storytelling, as recognized in the literature on film and animation theory. In this work, we take a particularly straightforward approach to providing the needed direction. Drawing on the observation that the cross-attention maps for prompt words reflect the spatial layout of objects denoted by those words, we introduce an optimization objective that produces “activation” at desired positions in these cross-attention maps. The resulting approach is a step toward generalizing the applicability of text-guided diffusion models beyond single images to collections of related images, as in storybooks. To the best of our knowledge, our Directed Diffusion method is the first diffusion technique that provides positional control over multiple objects, while making use of an existing pre-trained model and maintaining a coherent blend between the positioned objects and the background. Moreover, it requires only a few lines to implement.<sup>1</sup>

## 1 Introduction

Text-to-image models such as DALL·E 2 Ramesh et al. [2022], Imagen Saharia et al. [2022] and others have revolutionized image generation. Platforms such as Stable Diffusion hug [2023] and similar systems have democratized this capability, as well as presenting new ethical challenges.

The forementioned systems generate arbitrary images simply by typing a “prompt” or description of the desired image. It is not always highlighted, however, that experimentation and practical experience are often needed if the user has a particular result in mind. Text-to-image diffusion methods often fail to produce desired results, requiring repeated trial-and-error experiments with “prompt engineering” including negative prompts, different random seeds, and

---

<sup>1</sup>Our project page: <https://hohonu-vicml.github.io/DirectedDiffusion.Page>

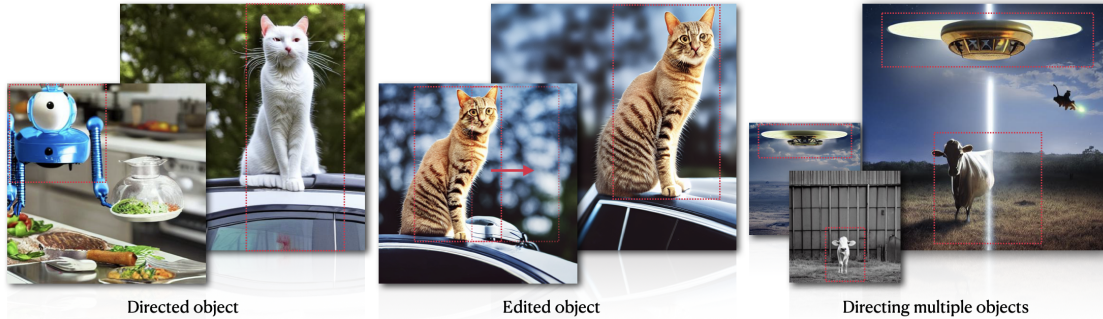


Figure 1: Directed Diffusion (DD) augments denoising diffusion text-to-image generation by allowing the position of specified objects to be controlled with user-specified bounding boxes (highlighted in red). (Left) DD generates specified objects (insect robot, cat) placed according to the given bounding boxes. We can move a synthesized object (middle), and place multiple objects in desired locations (right). All the directed objects show the appropriate “contextual” interaction (e.g. shadows) with the background. The prompts used in this figure, from left: “An insect robot preparing a delicious meal and food in the kitchen”, “A cat sitting on a car”, “A UFO abducting a cow with a light beam weapon.” Please enlarge figures to see details.

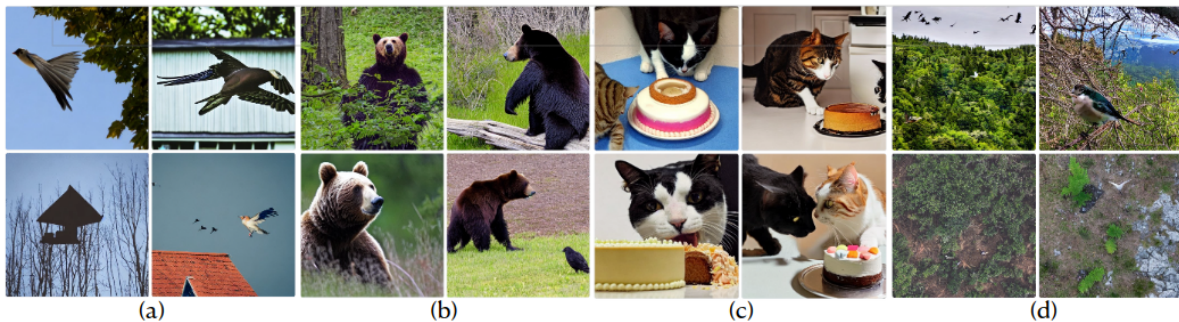


Figure 2: Stable Diffusion hug [2023] failure cases. (a) A bird flying over a house: no house, flying house. (b) A bear watching a bird: no bird, bear is not watching bird. (c) A cat watching a dog eat cake: cat is eating, no dog. (d) A nature photo with a bird in the upper left: “upper left” is ignored.

hyperparameters including the classifier-free guidance scale, number of denoising steps, and scheduler Smith [2022]. This is particularly true for complex prompts involving descriptions of several objects. For example, a prompt such as “a bird flying over a house” fails to generate the house with some seeds, and in other cases renders both the bird and house but without the “on” relationship (Fig. 2). The time required for experimentation is made worse if optimization or fine-tuning computation is required, especially on a per-image basis. These difficulties have led to the creation of “prompt marketplaces” pro [2023] where expert users share and sell successful settings.

The experimentation becomes prohibitive when the goal is to use the images for *storytelling*, since text-to-image methods offer no control over the required positioning of characters and objects. Prompts describing the content of an image do not indicate *where* objects should be placed, and indicating desired positions in the prompt usually fails (Figs. 1, 2). This is probably because the training data of text-image pairs is gathered from public sources, and people rarely annotate the location of objects in an image (“A photo of grandmother and her cat. Grandmother is in the center of the picture, and the cat is to her left.”) because it is generally obvious to the viewer. As a consequence, extensive and tedious repeated trials are needed to obtain an image where the desired objects exist and their randomly generated positions are acceptable.

A story generally involves a character interacting with the environment or with other characters. Conveying a story with images requires creating not just images with the desired semantic content, but images with objects in suitable relative *positions* (“The thief looked back at the princess before hurrying toward the door”). The subject of “Film Grammar” Arijon [1976] seeks to codify established principles for positioning characters relative to each other and the camera. Film Language guides include principles such as “To make things look natural, put lines, edges or faces about a third of the way across, up or down the picture ‘frame’. To make them look formal, put them in the middle; and to make things seem uncomfortable, make the shot unbalanced or put it at on a slant” <https://www.learnaboutfilm.com/> [2023]. The staging principle in traditional animation Thomas and Johnston [1981] similarly recognizes the importance of controlling the placement of characters and objects.

Research is addressing some limitations of text-guided diffusion methods, including methods that define new text tokens to denote specific and consistent character or object identities, provide mask-guided inpainting of particular regions, manipulate text guidance representations, and mitigate the common failure of guidance using CLIP-like models Radford et al. [2021] to understand the target of attributes such as colors. Existing methods still generally struggle to synthesize *multiple* objects with desired positional relationships (Section 5).

Our work is a further step toward guiding text-based diffusion, by introducing *coarse positional control for multiple objects* as needed for storytelling. In this application only *coarse* positional control is needed – for example a director might instruct an actor to “start from over there and walk toward the door”, rather than specifying the desired positions in floating point precision as is done in animation software packages. We take inspiration from the observation that position is established early in the denoising process Liew et al. [2022] and from the fact that the cross-attention maps have a clear spatial interpretation (see Fig. 3). Our general approach is to edit the cross-attention maps for particular words during the early denoising steps, so as to concentrate activation at the desired location of the object. We introduce an optimization objective that achieves this without disrupting the learned text-image association in the pretrained model and without requiring extensive code changes. See Section 3 for details. Our method is implemented using the Python Diffusers dif [2023] implementation of stable diffusion (SD) and makes use of the available pre-trained model.

Our method makes the following contributions:

- **Storytelling.** Our method is a first step towards storytelling by providing consistent control over the positioning of multiple objects.
- **Compositionality.** It provides a direct approach to “compositionality” by providing explicit positional control.
- **Consistency.** The positioned objects seamlessly and consistently fit in the environment, rather than appearing as a splice from another image with inconsistent interaction (shadows, lighting, etc.) This consistency is due to two factors. First, we use a simple bounding box to position and allow the denoising diffusion process to fill in the details, whereas specifying position with a pixel-space mask runs the risk that it may be inconsistent with the shape and position implicit in the early denoising results. Second, subsequent diffusion steps operate on the entire image and seamlessly produce consistent lighting, shadows, etc.
- **Simplicity.** Image editing methods for text-to-image models often require detailed masks, depth maps, or other precise guidance information. This information is not available when synthesizing images *ab initio*, and it would be laborious to create. Our method allows the user to control the desired locations of objects simply by specifying approximate bounding boxes. From a computational point of view, our method requires no fine tuning or other optimization, and can be added to an existing text-driven diffusion model with cross-attention guidance with only a few lines of code.

Storytelling also requires the ability to generate particular objects rather than generic instances (*this* cat rather than “any cat”), and our algorithm is complementary to methods Gal et al. [2022], Ruiz et al. [2022] that address this. For clarity, *the examples in the paper do not make use of these other algorithms.*

## 2 Related Work

Denoising diffusion models Sohl-Dickstein et al. [2015], Song and Ermon [2019], Ho et al. [2020], Song et al. [2021] add Gaussian noise to the data in a number of steps and then train a model to incrementally remove this noise. Aspects of the mathematics are presented in most papers and good tutorials are available Weng [2021], so we will simply mention several high-level intuitions. The end-result of the forward process is an image effectively consisting of independent normal distributed pixels, which is easy to sample. The backward process, denoises random samples from this distribution resulting in novel images (or other data). The mathematical derivation in Sohl-Dickstein et al. [2015], Ho et al. [2020] is somewhat similar to a hierarchical version of a VAE Kingma and Welling [2013], although with a fixed encoder and a “latent” space with the same dimensionality as the data. The fixed encoder provides an easy closed-form posterior for each step, allowing the overall loss to split into a sum over uncoupled terms for each denoising step, resulting in faster training. Song and Ermon [2019] introduced an alternate derivation building on score matching Hyvärinen [2005]. From this perspective adding noise is equivalent to convolving the probability density of the noise with the data, thus blurring the data distribution and providing gradients toward the data manifold from distant random starting points. The denoising process in Ho et al. [2020], Song and Ermon [2019] is stochastic, with an interpretation as Langevin sampling Song and Ermon [2019]. A deterministic variant, DDIM (Denoising Diffusion Implicit Models) was introduced in Song et al. [2021] and has advantages for editing applications.

Text-to-image models condition the image generation process on the text representation from joint text-image embedding models such as CLIP Radford et al. [2021], thereby providing the ability to synthesize images simply by typing a phrase

that describes the desired image. While text-to-image models have employed GANs as well as autoregressive models and transformers Patashnik et al. [2021], Yu et al. [2022], Chang et al. [2023], a number of recent successful approaches use diffusion models as the underlying image generation mechanism Nichol et al. [2022], Ramesh et al. [2022], Saharia et al. [2022]. This choice is likely motivated both by the stable training of these models and their ability to represent diverse multi-subject datasets. Among these systems, stable diffusion (SD) Rombach et al. [2022] has released both code and trained weights hug [2023] under permissive license terms, resulting in widespread adoption and a large ecosystem of related tools. This approach runs denoising diffusion in the latent space of a carefully trained autoencoder, providing accelerated training and inference. Stable diffusion implements classifier-free guidance using a cross-attention scheme. A projection of the latent image representation from SD’s U-net is used as the query, with projections of the CLIP embedding of the prompt supplying the key and value. While the key and value are constant, the query is changing across denoising steps, allowing it to iteratively extract needed information from the text representation Jaegle et al. [2021].

The literature on applications of diffusion models is difficult to fully survey, with many new papers appearing each week. A number of works have noted that the capabilities of text-guided diffusion can be extended with relatively simple modifications (sometimes requiring only a few lines of code). For the case of image editing, SDEdit Meng et al. [2022] runs a given image part way through the noising (forward) process and then denoises the result. This has an interpretation of “projecting on the image manifold”, and allows crude sketches to be denoised into sophisticated pictures. However there is a trade-off in the extent of the noising/denoising – using the full process “forgets” all knowledge of the input image and just produces an unrelated random sample, whereas denoising for too few steps stays close to the input guidance image and inherits any of its imperfections. Blended Diffusion Avrahami et al. [2022] uses a user-provided mask to blend a noised version of the background image with the CLIP-guided synthesized inpainted region at each step. The authors point out an analogy to classic frequency-selective pyramidal blending, with the low frequency features being merged earlier in the denoising process. Magicmix Liew et al. [2022] produces convincing novel images such as “*an espresso machine in the shape of a dog*”. Their technique simply starts the denoising process guided by the text prompt corresponding to the desired overall shape (“dog”) and switches to the prompt describing the content (“espresso machine”) at some step in the denoising process. This exploits the observation that the early denoising steps establish the overall position and shape of an object while the later steps fill in the “semantic details” (Fig. 3). Prompt-to-prompt Hertz et al. [2022] demonstrates that powerful text-driven image editing can be obtained by substituting or weighting the cross-attention maps corresponding to particular words in the prompt. The paper also clearly illustrated the fact that the cross-attention maps have a spatial interpretation. Structured diffusion guidance Feng et al. [2022] addresses the attribute binding problem in which text-to-image models often fail to associate attributes such as colors with the correct objects. Their approach parses the prompt to obtain noun phrases with their associated attributes, and then these additional text embeddings are combined with that for the original prompt in generating the cross-attention. Other research goes beyond manipulations of pre-trained diffusion models by introducing optimization or fine tuning to produce additional effects Ruiz et al. [2022], Yang et al. [2022], Valevski et al. [2022], Kawar et al. [2022].

Closer to our work, Liu et al. [2022] merges the results of denoising guided by multiple prompts using conjunction and negation operations. This method reliably produces images composed of multiple text prompts with different subjects (a common failure case of text-to-image models), but provides no positional control over the elements. We approach this problem more directly, by specifying the position of multiple objects through their corresponding attention maps. Concurrent with our work, Park et al. [2022] demonstrate high-quality inpainting driven by a combination of text and detailed masks. They edit the cross-attention map for the subject to be inpainted to correspond to a low-resolution version of the mask. This addresses a problem with some mask-based editing methods where the shape of the mask can be inconsistent with the shape implicitly defined by the early noise layout, thus resulting in poor alignment of the synthesized region to the mask. Our work also uses editing of the cross attention maps, but we inject activation in the desired spatial region to guarantee it is non-zero. Our method does not have an issue with mask vs. noise alignment since masks are not used. We also target full synthesis rather than inpainting. The work Pan et al. [2022] introduces an alternate approach to synthesizing images for storytelling, using an autoregressive formulation of latent diffusion in which each new image is conditioned on previous captions and images. This approach produces good results when given caption fragments that are interpretable in the context of the preceding captions and images. The positions of subjects are not controlled, however, making it difficult to satisfy position-based storytelling principles.

### 3 Methods

Our objective is to create a controllable synthetic image from a text-guided diffusion model without any training by manipulating the attention from cross-attention layers, and the predictive latent noise. We use the following notation: Bold capital letters (e.g.,  $M$ ) denote a matrix or a tensor, vectors are represented with bold lowercase letters (e.g.,  $\mathbf{m}$ ),

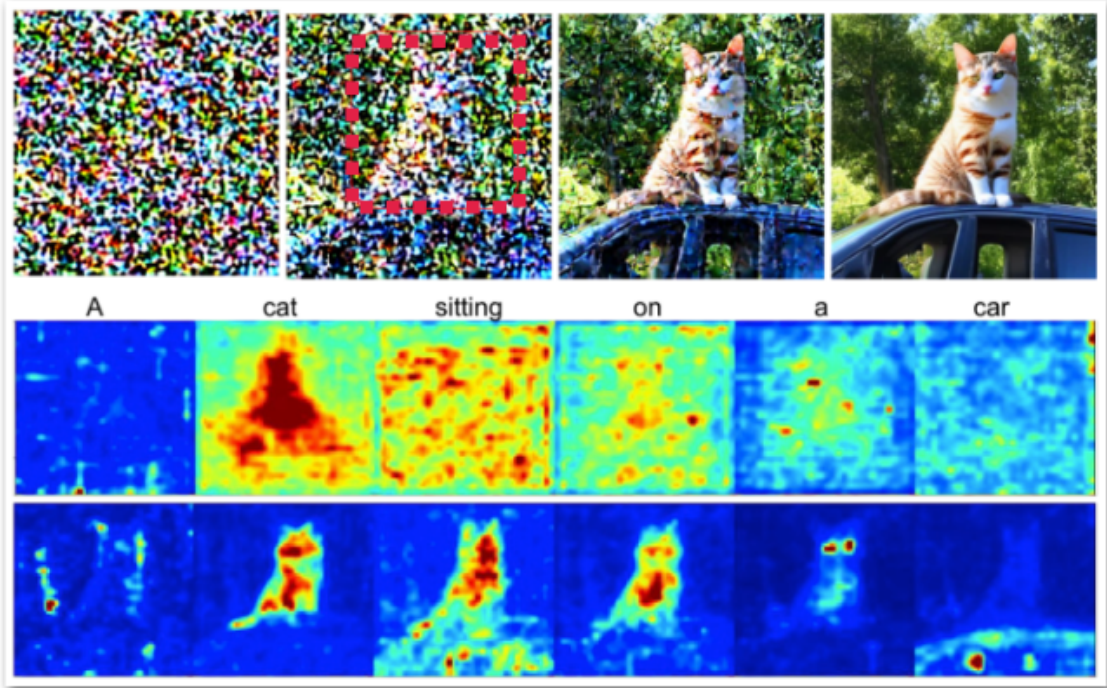


Figure 3: (Top, from left to right): The reverse SD denoising process from the initial stage to the end of process. Note that the position of the cat is evident early in the process (red box), however the details that define it as a cat are not yet clear. (Bottom): The cross-attention maps associated with each word in the prompt, where the first and second row are from the first denoising step, and the final step, respectively. The cat’s shape is clearly visible in the cross-attention maps for the word "cat" (and in the maps for "sitting" and "on" in the final step).

and lowercase letters (e.g.,  $m$ ) denote scalars. Depending on the context, the superscript  $i$  on a three-dimensional tensor (e.g.,  $\mathbf{M}^{(i)}$ ) denotes a tensor slice (a matrix). In this section, this index specifies the slice of the cross-attention map associated with a particular token in the prompt. Similarly,  $\mathbf{M}^{(i:j)}$  denotes the stacked slices  $i$  to  $j$  of the tensor.

The DD procedure controls the placement of objects corresponding to several groups of selected words in the prompt; we refer to these as *directed objects* and *directed prompt words* respectively. DD builds on SD Rombach et al. [2022] and it is assumed that the reader is familiar with that work.

Our method is inspired by the intermediate result shown in Fig. 3 (Top). As shown in this figure, the overall position and shape of a synthesized object appears near the beginning of the denoising process, while the final denoising steps do not change this overall position but add details that make it identifiable as a particular object (cat). This observation has also been exploited in previous work such as Liew et al. [2022].

An additional phenomenon can be found in the cross-attention maps, as shown in Fig. 3 (bottom two rows). The cross-attention map has a spatial interpretation, which is the “correlation” between locations in the image and the meaning of a particular word in the prompt. For instance, we can see the cat shape in the cross-attention map associated with the word “cat”. DD utilizes this key observation to spatially guide the diffusion denoising process to satisfy the user’s requirement.

### 3.1 Pipeline

Given the prompt  $\mathcal{P}$  and the associated region information  $\mathcal{R}$  indicating the directed objects, DD synthesizes an image  $\mathbf{x}_0$  with appropriate “contextual interaction” between the objects and the remainder of the scene. It uses a pre-trained Latent Diffusion Model (LDM) Smith [2022] no further fine-tuning. The region information  $\mathcal{R}$  comprises a set of parameters  $\mathcal{R} = \{\mathcal{B}, \mathcal{I}\}$ , denoting the bounding boxes to position the directed objects, and the directed prompt word indices in the prompt. We will describe these in Sec. 3.2.

Following conventional notation, we define  $\mathbf{x}_t$  and  $\mathbf{z}_t$  as the synthesized SD image and the predicted latent noise at time step  $t$ , respectively, where  $t \in \{T, \dots, 0\}$  in the denoising fashion. The images  $\mathbf{x}_t$  are reconstructions obtained by

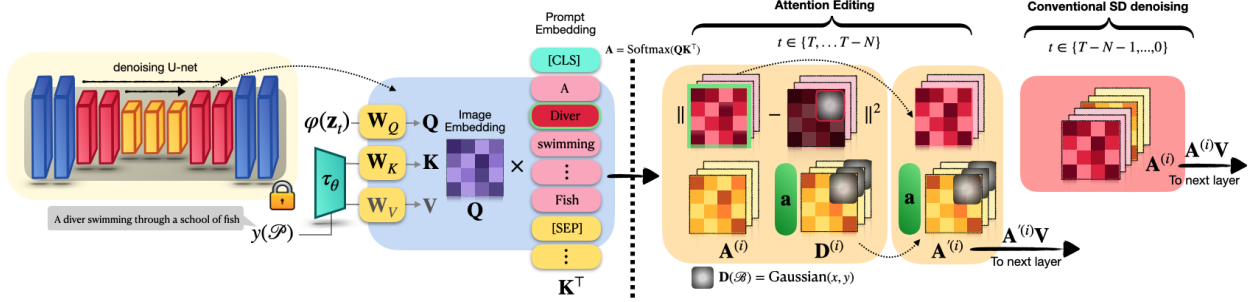


Figure 4: Directed Diffusion (DD) pipeline overview: DD divides the denoising process into initial steps where *Attention Editing* is performed, followed by refinement steps using *Conventional SD Denoising*. The goal of the *Attention Editing* stage is to optimize the cross attention map for a directed word (red, outlined in green) to approximately match a target  $\mathbf{D}$  in which neural “activation” has been injected with a Gaussian fall-off inside a bounding box specified by the user. The optimization is performed by adjusting a vector ( $\mathbf{a}$ , green) that re-weights the trailing attention maps. Note that the optimization objective involves two time steps. Please see the text for details.

feeding the latent  $\mathbf{z}_t$  through the VAE decoder  $\mathcal{D}(\cdot)$ . The images  $\mathbf{x}_T$  and  $\mathbf{x}_0$  correspond to the Gaussian noise latent  $\mathbf{z}_T$  and the final predicted latent  $\mathbf{z}_0$ , respectively.

The principle of this work is based on the concept “*first position the objects, then refine the results*”. This is reflected in the overall Directed Diffusion pipeline shown in Fig. 4 and also the applications detailed in Sec. 4.

*Attention Editing.* From a high-level perspective, this stage focuses on spatially editing the cross-attention map used for conditioning in stable diffusion. It operates during the diffusion steps  $t \in [T, T - N]$  that establish the object location, where  $N$  is a hyperparameter determining the number of steps in this stage. We chose  $N = 10$  in most of our experiments. As described in Sec. 3.2, this stage modifies the cross-attention map during the first  $N$  denoising steps by amplifying the region inside  $\mathcal{B}$  while down-weighting the surrounding areas through optimization (the upper path to the yellow regions in Fig. 4).

*Conventional SD Denoising.* Following the attention editing stage, this stage runs the standard SD process using classifier-free guidance Ho and Salimans [2021] over the remainder of the reverse diffusion denoising steps  $t \in \{T - N, \dots, 0\}$ . Note that the only difference between the two stages is the cross-attention editing (the lower path to the red region in Fig. 4).

### 3.2 Cross-Attention Map Guidance

To achieve our goal, DD asks the user specific information about the “direction” of the object with  $\mathcal{R} = \{\mathcal{B}, \mathcal{I}\}$  to guide the denoising SD process, where  $\mathcal{B}$  and  $\mathcal{I}$  denote the bounding box specification and the directed prompt words indices in  $\mathcal{P}$ , respectively. We will use the prompt “*A bear watching a flying bird*” as our specific example throughout this section and the next section.

Specifically, a bounding box  $\mathcal{B} = \{(x, y) \mid b_{\text{left}} \times w \leq x \leq b_{\text{right}} \times w, b_{\text{top}} \times h \leq y \leq b_{\text{bottom}} \times h\}$  is the set of all pixel coordinates inside the bounding box of resolution  $w \times h$ . The bounding box with label  $i$  guides the location of the subject indicated by the  $i$ th prompt word. The exact location and shape of the subject results from the interaction of the Gaussian activation window inside this box with the activation  $\mathbf{z}_i$  in the U-net, hence the object is not restricted in shape and may extend somewhat outside the box. In our implementation,  $\mathcal{B}$  is generated based on a tuple of four scalars representing the boundary of the bounding box, denoted as  $\mathbf{b} = (b_{\text{left}}, b_{\text{right}}, b_{\text{top}}, b_{\text{bottom}})$ , where  $b_{\text{left}}, b_{\text{right}}, b_{\text{top}}, b_{\text{bottom}} \in [0, 1]$  describe the bounding box of the directed object position expressed as fractions of the image size,

SD implements text-guided synthesis with classifier-free guidance using cross-attention between the projected embedding  $\mathbf{Q}$  of the SD latent  $\mathbf{z}_t$  and the projected embeddings  $\mathbf{K}$  of the  $|\mathcal{W}|$  potential words from the prompt. The product  $\mathbf{Q}\mathbf{K}^T \in \mathbb{R}^{n^2 \times |\mathcal{W}|}$  (following a softmax and normalization) can be interpreted as  $|\mathcal{W}|$  individual cross-attention maps  $\mathbf{A}^{(i)}$  (see Fig. 3, bottom), each having a spatial interpretation of an  $n \times n$  image. SD uses CLIP Radford et al. [2021] as its text encoder, which has  $|\mathcal{W}| = 77$ , while  $n = 64$ , matching the latent spatial dimension in the current SD implementation. The cross-attention maps  $\mathbf{A}^{(i)}$  are divided into a subset of *prompt maps*  $\mathbf{A}^{(i)}$ ,  $1 \leq i \leq |\mathcal{P}|$  corresponding to words in the prompt, and the remainder  $i \in \mathcal{T}$  where  $\mathcal{T} := \{|\mathcal{P}| + 1, \dots, |\mathcal{W}|\}$  that do not correspond to any words but are computed to allow constant-size matrix computations. We term the latter as *trailing attention maps*. We denote the prompt words for an object to be directed with an indices set  $\mathcal{I} \subset \{i \mid i \in \mathbb{N}, 1 \leq i \leq |\mathcal{P}|\}$ . For the bear example,  $\mathcal{I} = \{1, 2\}$  to denote “A” and “bear” in the prompt.

We wish to edit the cross attention maps corresponding to the “directed” words in the prompt so as to place the object at the bounding box. In one initial experiment, we used an optimization objective that encouraged the latent variables  $\mathbf{z}_t$  to have high energy in the desired region during the attention editing steps. This was not stable, which might be explained by the fact that it is potentially pushing  $\mathbf{z}_t$  outside the range of values encountered during training.

Thus, we wish to guide the directed cross-attention maps, but without disrupting the image-text relationship that is learned during training. One strategy is to use the network itself to project the solution near the “trained manifold”, by expressing an objective at time  $t$  in terms of coarser guidance made at time  $t + 1$  that is refined during the  $t + 1 \rightarrow t$  denoising step. Another observation is that we can separate the desired coarse guidance from the directed cross attention maps by making use of the trailing maps to express the coarse guidance, since these are also included in the  $\mathbf{QK}^T$  product.

Given  $\mathcal{B}$ , we generate a modified cross-attention map using two functions:

$$\text{WeakenMask}(\mathcal{B}')_{xy} = \begin{cases} 1, & (x, y) \in \mathcal{B}' \\ c, & \text{otherwise,} \end{cases}$$

$$\text{StrengthenMask}(\mathcal{B})_{xy} = \begin{cases} f(x, y), & (x, y) \in \mathcal{B} \\ 0, & \text{otherwise,} \end{cases}$$

where  $\mathcal{B}'$  is the complement of  $\mathcal{B}$ , and  $f(\cdot)$  denotes the function that “injects attention” to amplify the region  $\mathcal{B}$ . In our implementation, we use a Gaussian window of size  $\sigma_x = b_w/2, \sigma_y = b_h/2$  to generate the corresponding weight, where  $b_w = \text{ceil}((b_{\text{right}} - b_{\text{left}}) \times w), b_h = \text{ceil}((b_{\text{top}} - b_{\text{bottom}}) \times h)$  are the width and the height of  $\mathcal{B}$ .

The  $\text{WeakenMask}(\cdot)$  and  $\text{StrengthenMask}(\cdot)$  functions “direct” selected subjects from the prompt toward specific locations of the image in the SD denoising process.  $\text{StrengthenMask}(\cdot)$  inserts higher activation into the provided bounding box with a Gaussian window, while  $\text{WeakenMask}(\cdot)$  attenuates the region outside  $\mathcal{B}$  by multiplying by  $c < 1$ .

The resulting edited maps  $\mathbf{D}^{(i)}$  are termed *target* maps. They are not used directly in the cross-attention denoising guidance. Instead, as described next,  $\mathbf{D}^{(i)} \forall i \in \mathcal{I}$  provide a target for the loss in Eq. 1, while  $\mathbf{D}^{(i)} \forall i \in \mathcal{T}$  are un-weighted sources for the weighted trailing maps created in Algo. 1 line 12.

---

#### Algorithm 1 DD Cross-Attention Editing Algorithm

---

```

1: Input: A diffusion model  $\text{DM}(\cdot)$ , prompt  $\mathcal{P}$ , directions  $\mathcal{R} = \{\mathcal{B}, \mathcal{I}\}$ , current step  $t$ 
2: Output: Predicted conditional noise  $\mathbf{z}_{\text{cond}}$  at time  $t$  from  $\text{DM}(\cdot)$ 
3: Parameters: Gaussian weighting scalar  $c_g$ 
4: procedure DDCROSSATTNEDIT( $\text{DM}(\cdot), \mathcal{P}, \mathcal{B}$ )
5:   for  $l \in \text{layer}(\text{DM}(\mathbf{z}_t, \mathcal{P}))$  do
6:     if  $\text{type}(l) \in \text{CrossAttn}$  then
7:        $\mathbf{A} = \text{Softmax}(\mathbf{Q}_l(\mathbf{z}_t) \cdot \mathbf{K}_l(\mathcal{P})^T)$ 
8:        $\mathbf{W} \leftarrow \text{WeakenMask}(\mathcal{B}')$ 
9:        $\mathbf{S} \leftarrow \text{StrengthenMask}(\mathcal{B})$ 
10:       $\mathbf{D}^{(i)} \leftarrow \mathbf{A}^{(i)} \odot \mathbf{W} + \cdot \mathbf{S} \quad \forall i \in \mathcal{T} \cup \mathcal{I}$ 
11:       $\mathbf{a}^* := \arg \min_{\mathbf{a}} \mathcal{L}_{\mathbf{a}}$ 
12:       $\mathbf{A}'^{(|\mathcal{P}|+1:77)} := \text{Diag}(\mathbf{a}^*) \odot \mathbf{D}^{(|\mathcal{P}|+1:77)}$ 
13:       $\mathbf{z}_t \leftarrow l(\mathbf{z}_t, \mathbf{A}' \cdot \mathbf{V}_l(\mathcal{P}))$ 
14:     else
15:        $\mathbf{z}_t \leftarrow l(\mathbf{z}_t)$ 
16:     end if
17:   end for
18:   return  $\mathbf{z}_t$ 
19: end procedure

```

---

Algo. 1 is the core of DD. SD implements denoising with a U-net architecture, where text guidance  $\tau_\theta(y(\mathcal{P}))$  from the prompt is passed to layers of the U-net through cross-attention layers, with  $y(\cdot)$  and  $\tau_\theta(\cdot)$  denoting the tokenizer and text embedding, respectively. In each of these cross attention layers, DD clones and modifies selected cross-attention maps  $\mathbf{A}^{(i)}, \forall i \in \mathcal{I} \cup \mathcal{T}$  to form the target maps  $\mathbf{D}$  (line 10) for the optimization objective (line 11, Eq. 1).

Our optimization objective seeks to find the best weighed combination of the trailing maps at time  $t$ , by means of a learned weight vector  $\mathbf{a} \in \mathbb{R}^{77-|\mathcal{P}|-1}$ , such that the “directed” prompt maps  $\mathbf{A}^{(i)}, i \in \mathcal{I}$  best match the corresponding

target maps  $\mathbf{D}^{(i)}$  (with some abuse of notation):

$$\mathcal{L}_{\mathbf{a}_t} = \sum_i \|\mathbf{A}_{t-1}^{(i)} \left( \mathbf{A}_t^{(|\mathcal{P}|+1:77)} \cdot \text{Diag}(\mathbf{a}_t) \right) - \mathbf{D}^{(i)}\|^2, \quad (1)$$

$$\forall i \in \mathcal{I}, \forall t \in \{T, \dots, T - N\},$$

where the notation  $\mathbf{A}_{t-1}^{(i)}(\cdot)$  indicates an (indirect) *functional* dependence of the cross-attention map at time  $t - 1$  on the weighted sum of the trailing maps edited at time  $t$ . After the weights  $\mathbf{a}^* = \arg \min_{\mathbf{a}} \mathcal{L}_{\mathbf{a}_t}$  are obtained (line 11), they are used to produce re-weighted trailing maps  $\mathbf{A}'$  (line 12), which then influence the overall cross-attention conditioning at time  $t$  (line 13).

To summarize the dependency flow, the trailing maps at time  $t$  are edited, and are reweighted by the optimized  $\mathbf{a}$ . These then influence the denoising at time  $t$ , which in turn influences the cross attention map at time  $t - 1$ . This dependency structure involving expressing the loss at time  $t - 1$  is necessary because at time  $t$  the loss does not involve the weights  $\mathbf{a}$ , resulting in a zero gradient. In addition we believe that influencing the desired cross-attention through an intermediate denoising step helps keep the solution closer to states seen in training and thus removes the instability we found when directly optimizing for  $\mathbf{z}_t$ . Please refer to the Appendix for further implementation details.

## 4 Applications

This section demonstrates two applications that can be utilized following the DD reconstruction process. Both methods re-use information recorded from the DD processes. In the descriptions, recall that in SD algorithms the latent  $\mathbf{z}_t$  ( $64 \times 64$  in current implementations) has direct a spatial interpretation.

### 4.1 Scene compositing

Composing multiple objects is a challenging problem in image generation. Complex prompts involving a relation between two objects (“bear watching bird”) often fail in current text-to-image models (Fig. 2). While our DD pipeline supports the direction of multiple objects by means of multiple bounding boxes  $\mathcal{B}$ , in practice, the results are unreliable when the number of bounding boxes is more than two. We resolve this problem by additional editing operations.

Specifically, we first use DD to individually generate multiple objects, and record the latent information  $\mathbf{z}_t^{(r)}$  of all steps for the directed objects  $r \in \{1, \dots, R\}$ , where  $R$  is the total number of directed objects. Then, inspired by Liu et al. [2022], we sum and average the linear interpolation of the  $\mathbf{z}_t^{(r)}$  and the latent conditioned on the original prompt  $\mathcal{P}$ ,

$$\mathbf{z}_t := \frac{1}{R} \sum_r w_r \times \mathbf{z}_t + (1 - w_r) \times \mathbf{z}_t^{(r)}, \quad \forall t \in \{T, \dots, T - N\}, \quad (2)$$

where the  $w_r \in \mathbb{R}$  is a given weight, generally set to 0.1 in our experiments. After  $N$  steps of applying Eq. 2 ( $N \approx 10$ , see supplementary), SD is used to refine the result and produce contextual interactions.

### 4.2 Placement Finetuning

In some cases the artist may wish to experiment with different object positions after obtaining a desirable image. However, when the object’s bounding box is moved DD may generate a somewhat different object. Our placement finetuning (PF) method addresses this problem, allowing the artist to immediately experiment with different positions for an object while keeping its identity, and without requiring any model fine-tuning or other optimization Gal et al. [2022], Ruiz et al. [2022]. Note that the PF method is not intended to produce a sequence of images for a video, as that would generally require further control over 3D object pose, camera viewpoint, etc.

Fig. 5 illustrates the placement finetuning algorithm. The algorithm has three components. First (Fig. 5, top), a mask  $\mathbf{M}_o$  for the directed object is obtained by thresholding the final  $t = 0$  cross-attention computed by DD and clipping by the bounding box  $\mathcal{B}$ . At a selected time step  $T - N$  the transformation  $X(\cdot)$  is applied to the recorded latent  $\mathbf{z}_{T-N}$ , and to the mask  $\mathbf{M}_o$ , producing a translated mask  $X(\mathbf{M}_o)$ . A mask  $\neg\mathbf{M}_o$  is computed as the complement of  $\mathbf{M}_o$  and is used to extract the background region for an initial placement-finetuned latent  $\mathbf{z}'_{T-N}$ .

The second component (not shown in the figure) inpaints holes in the background caused by moving the foreground object. These hole regions are initialized with the transformed latent  $X(\mathbf{z}_T)$  masked by  $\mathbf{M}_o$ . In our experiments the transformation  $X(\cdot)$  is translation implemented with `torch.roll`, which causes content that is translated beyond the tensor dimension to wrap around and re-appear on the opposite side. This has the effect of initializing the hole

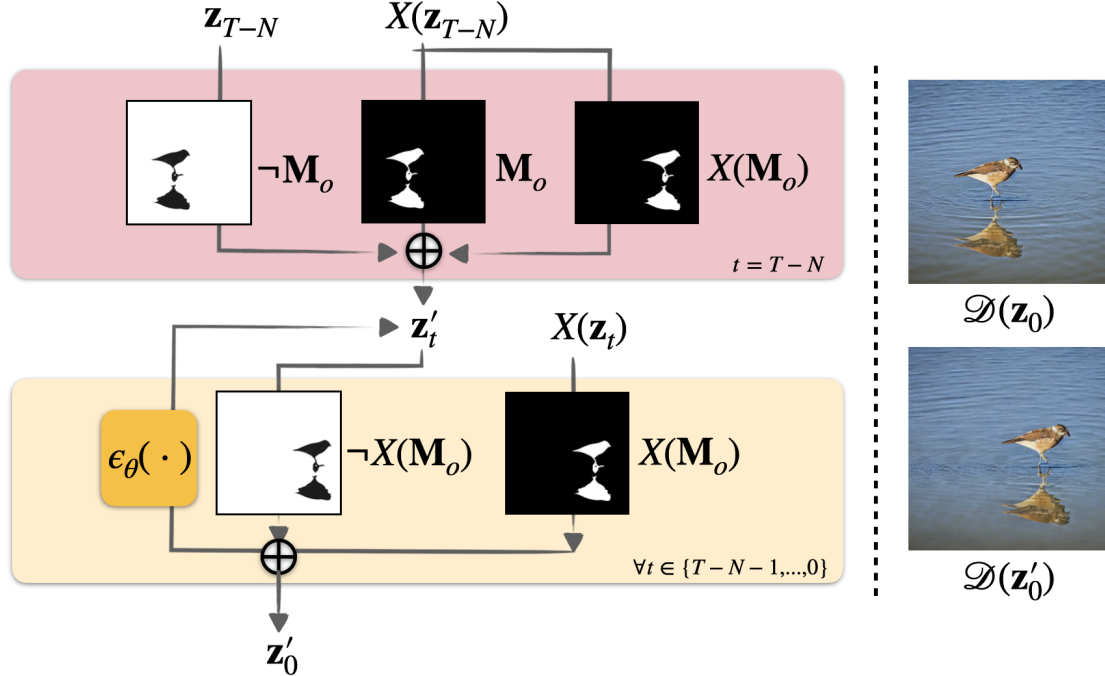


Figure 5: Placement finetuning. The final ( $t=0$ ) cross-attention map recorded from a previous DD synthesis is segmented into foreground and background. At a chosen editing time step  $T - N$  the foreground is moved and the background is inpainted. This edited latent is then further denoised to produce a coherent image. See the text for details.

that would otherwise appear on the opposite side with somewhat reasonable values, however more sophisticated inpainting schemes are possible here. After these initializations we perform a single iteration of adding noise followed by denoising, in order to cause the inpainted areas to have distinct detail and blend with the background.

Lastly, (Fig. 5, bottom) there are  $T - N - 1$  steps in which the transformed latent from the current step is composited with the background,

$$\mathbf{z}'_t := \mathbf{z}'_t \odot \neg X(\mathbf{M}_o) + X(\mathbf{z}_t) \odot X(\mathbf{M}_o), \quad \forall t \in \{T - N - 1, \dots, 0\}.$$

followed by denoising, resulting in a coherent refined image. The editing time step is generally set at  $N = 10$  in our experiments (see supplementary). Large  $N$  better preserves the original foreground and background, while smaller  $N$  encourages more interaction between the foreground and background.

Fig. 5 (right) shows the reconstruction of the latent image before and after transformation. The bird is successfully repositioned while maintaining coherent interaction with the background (reflection, waves).

## 5 Experiments

We now present example results of Directed Diffusion. As described earlier, unmodified text-to-image methods such as stable diffusion are fallible and may fail to correctly portray objects mentioned in the prompts. We inherit this variability, and the results shown here are representative but not guaranteed. Please see the supplementary for several additional results.

Fig. 6 shows examples of directing objects to lie in each of four image quadrants as well as at the image center, with the directed objects “a large cabin”, “an insect robot”, and “the sun”. Notice for example that the “sun” examples show the effect of the sun in the correct quadrant but in different contexts. The 3rd quadrant and the center show the real sun at the edge of the house roof, while the other images show the reflection of the sun such as from a window (e.g., 1st, 4th quadrant), or the wall (e.g., 2nd quadrant).

Fig. 7 shows the result of moving an object from left to right. All the results are generated with a bounding box with the full image height and 40% of the image width. The directed objects are “a stone castle”, “a white cat”, and “a white dog”, respectively.

Fig. 8 shows two experiments each with two directed objects: Fig. 8 (top) directs the objects “red cube”, “blue sphere”, while Fig. 8 (bottom) shows “bear”, “bird”, respectively. This is the well known “compositionality” failure case for

SD,<sup>2</sup>, however, DD is able to handle this case. Additionally, unlike Liu et al. [2022], which addresses this problem using a specifically trained model in their polygons example, we are able to use the generic pre-trained SD model without further modification. This results in our backgrounds having a variety of natural textures correctly aligned with the prompt contextual information (for example, the shadow of the blue sphere). In addition, the correlation of the directed objects is also retained, such as the “*watching*” prompt word associated with the bear and the bird.

Fig. 9 shows results of the placement finetuning method. Fig. 9 (bottom) revisits the sliding window castle experiment from Fig. 7. Using PF, the castle identity is preserved, while the surrounding environment such as the trees and lake reflection are reasonably synthesized.

## 6 Limitations and Conclusion

### 6.1 Limitations

Directed Diffusion inherits most of the limitations of stable diffusion, including the need for trial-and-error exploration over the prompt, random seeds, and hyperparameters (Fig. 2). Some random seeds fail to produce the desired subject or produce distorted objects such as animals with missing limbs. With a prompt such as *a horse in front of a castle*, placing the horse near the top of the image often fails. We believe this is because typical training images show the horse on the ground with the camera somewhat parallel to the ground plane. In common with methods such as Meng et al. [2022], Liew et al. [2022], it is necessary to specify the number of steps over which editing is active. While our method allows the position of specified objects to be controlled, it does not offer control over the orientation of the objects. This requirement comes up in a film language principle that “an actor on a journey should be portrayed in a consistent orientation.”

### 6.2 Conclusion

Storytelling with images requires directing the *placement* of important objects in each image. Our algorithm, directed diffusion, is a first step toward this goal. The algorithm is simple to implement, requiring only a few lines of code modification of a widely used library dif [2023]. The algorithm has significant limitations, in particular (and in common with many other text-to-image methods) there is a need to experiment with prompts and hyperparameters. Significant additional advances will be needed before video storytelling is possible. However, our method may be sufficient for the creation of storybooks, comic books, etc. when used in conjunction with other diffusion image guidance and editing techniques.

This paper continues a graphics research tradition in which an artist is guiding and interacting with generative tools. On the other hand, recent advances in generative models (of both images and text) suggest that a future in which anyone can make a movie using only high level direction (“make me a comedy movie about a cat that saves the world by ...”) is no longer science fiction. Several factors suggest this future is still distant, however. For one, the overall generation of stories is not a fully solved problem. This includes aspects such as the narrative arc and synthesis of the film language needed to convey the story to a viewer. Second, neural video generation experiments generally trade spatial for temporal resolution due to memory limits, and current results generally show a few seconds of video at fairly low resolution (recall that mainstream movies are 4K resolution), while sometimes suffering from flickering and distorted objects. In conclusion, there remains a role for artist-directed graphics in the near future.

## 7 Acknowledgements

We thank Jason Baldrige and Arkanath Pathak for helpful feedback.

## References

- Aditya Ramesh, Prafulla Dhariwal, Alex Nichol, Casey Chu, and Mark Chen. Hierarchical text-conditional image generation with CLIP latents. *CoRR*, abs/2204.06125, 2022.
- Chitwan Saharia, William Chan, Saurabh Saxena, Lala Li, Jay Whang, Emily Denton, Seyed Kamyar Seyed Ghasemipour, Burcu Karagol Ayan, S. Sara Mahdavi, Rapha Gontijo Lopes, Tim Salimans, Jonathan Ho, David J. Fleet, and Mohammad Norouzi. Photorealistic text-to-image diffusion models with deep language understanding. *CoRR*, abs/2205.11487, 2022.

<sup>2</sup>This failure case is highlighted on the huggingface hug [2023] stable diffusion website <https://huggingface.co/CompVis/stable-diffusion-v-1-1-original>



Figure 6: Four quadrants: (Top) Prompt: “A large cabin on top of a sunny mountain in the style of Dreamworks artstation”, with the directed object “a large cabin”. (Middle) Prompt: “An insect robot preparing a delicious meal and food in the kitchen”, with the directed object “an insect robot”. (Bottom) Prompt: “The sun shines on a house”, with the directed object “the sun”. Images from the left are SD, DD(1st Q), DD(2nd Q), DD(3rd Q), and DD(4th Q), respectively, where Q denotes the directed quadrant.

Stable diffusion 1 demo. <https://huggingface.co/spaces/stabilityai/stable-diffusion-1>, 2023. Accessed: 2023-01-01.

E. Smith. A traveler’s guide to the latent space, 2022. URL <https://www.notion.so/A-Traveler-s-Guide-to-the-Latent-Space-85efba7e5e6a40e5bd3cae980f30235f>.

Best stable diffusion prompts for ai art; top 5 list marketplaces, 2023. URL <https://csform.com/best-prompt-marketplaces-for-ai-art>.

Daniel Arijon. *Grammar of the Film Language*. Focal Press, 1976.

<https://www.learnaboutfilm.com/>. Telling your story: Film language for beginner filmmakers, 2023. URL <https://www.learnaboutfilm.com/film-language>.

Frank Thomas and Ollie Johnston. *Disney animation : the illusion of life*. Abbeville Press New York, 1st ed. edition, 1981. ISBN 0896592332 0896592324.

Alec Radford, Jong Wook Kim, Chris Hallacy, Aditya Ramesh, Gabriel Goh, Sandhini Agarwal, Girish Sastry, Amanda Askell, Pamela Mishkin, Jack Clark, Gretchen Krueger, and Ilya Sutskever. Learning transferable visual models from natural language supervision. In *Proc. ICML*, 2021.

Jun Hao Liew, Hanshu Yan, Daquan Zhou, and Jiashi Feng. Magicmix: Semantic mixing with diffusion models. *CoRR*, abs/2210.16056, 2022.

Diffusers library, 2023. URL <https://github.com/huggingface/diffusers>.

Rinon Gal, Yuval Alaluf, Yuval Atzmon, Or Patashnik, Amit H. Bermano, Gal Chechik, and Daniel Cohen-Or. An image is worth one word: Personalizing text-to-image generation using textual inversion. *CoRR*, abs/2208.01618, 2022.

Nataniel Ruiz, Yuanzhen Li, Varun Jampani, Yael Pritch, Michael Rubinstein, and Kfir Aberman. Dreambooth: Fine tuning text-to-image diffusion models for subject-driven generation. *CoRR*, abs/2208.12242, 2022.

Jascha Sohl-Dickstein, Eric Weiss, Niru Maheswaranathan, and Surya Ganguli. Deep unsupervised learning using nonequilibrium thermodynamics. In *International Conference on Machine Learning*, 2015.

Yang Song and Stefano Ermon. Generative modeling by estimating gradients of the data distribution. In *NeurIPS*, volume 32, 2019.

Jonathan Ho, Ajay Jain, and Pieter Abbeel. Denoising diffusion probabilistic models. *Advances in Neural Information Processing Systems*, 33, 2020.

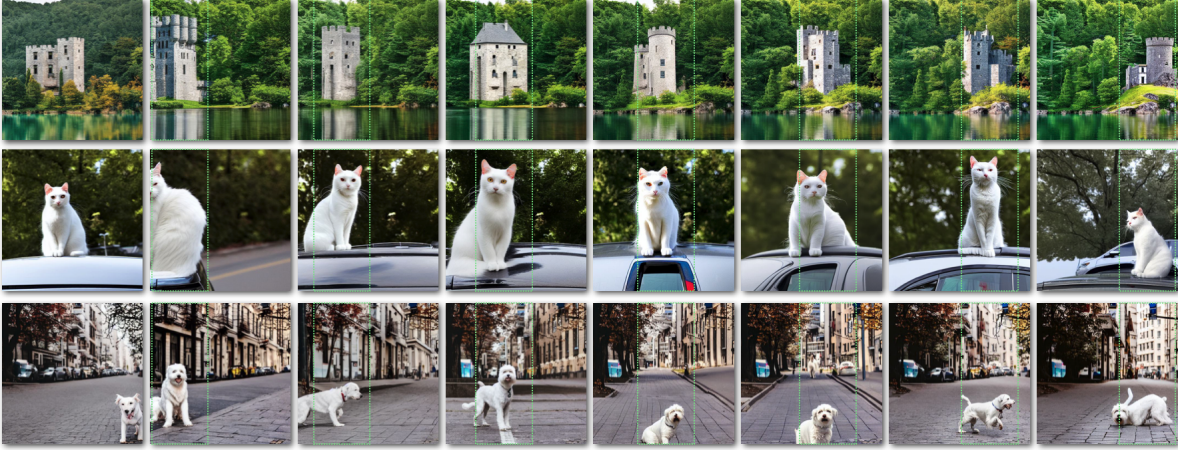


Figure 7: Sliding window: (Top) Prompt: “A stone castle surrounded by lakes and trees”, with the directed object “A stone castle”. (Middle) Prompt: “A white cat sitting on a car”, with the directed object “A white cat”. (Bottom) Prompt: “A white dog waking on the street in the city”, with the directed object “A white dog”. From the left: SD,  $DD_h(0\%, 40\%)$ ,  $DD_h(10\%, 50\%)$ ,  $DD_h(20\%, 60\%)$ ,  $DD_h(30\%, 70\%)$ ,  $DD_h(40\%, 80\%)$ ,  $DD_h(50\%, 90\%)$ ,  $DD_h(60\%, 100\%)$ , where  $DD_h(\cdot, \cdot)$  denotes the left and right edge of the directed region, expressed as percentages of the image resolution.

Jiaming Song, Chenlin Meng, and Stefano Ermon. Denoising diffusion implicit models. In *9th International Conference on Learning Representations, ICLR 2021, Virtual Event, Austria, May 3-7, 2021, 2021*.

Lilian Weng. What are diffusion models?, 2021. URL <https://lilianweng.github.io/posts/2021-07-11-diffusion-models/>.

Diederik P Kingma and Max Welling. Auto-encoding variational bayes. *arXiv preprint arXiv:1312.6114*, 2013.

Aapo Hyvärinen. Estimation of non-normalized statistical models by score matching. *J. Mach. Learning Research*, 6: 695–709, 2005.

Or Patashnik, Zongze Wu, Eli Shechtman, Daniel Cohen-Or, and Dani Lischinski. Styleclip: Text-driven manipulation of stylegan imagery. In *ICCV*, 2021.

Jiahui Yu, Yuanzhong Xu, Jing Yu Koh, Thang Luong, Gunjan Baid, Zirui Wang, Vijay Vasudevan, Alexander Ku, Yinfei Yang, Burcu Karagol Ayan, Ben Hutchinson, Wei Han, Zarana Parekh, Xin Li, Han Zhang, Jason Baldridge, and Yonghui Wu. Parti: Pathways autoregressive text-to-image model, 2022. URL <https://github.com/google-research/parti>.

Huiwen Chang, Han Zhang, Jarred Barber, Aaron Maschinot, José Lezama, Lu Jiang, Ming-Hsuan Yang, Kevin Murphy, William T. Freeman, Michael Rubinstein, Yuanzhen Li, and Dilip Krishnan. Muse: Text-to-image generation via masked generative transformers. *CoRR*, abs/2301.00704, 2023.

Alexander Quinn Nichol, Prafulla Dhariwal, Aditya Ramesh, Pranav Shyam, Pamela Mishkin, Bob McGrew, Ilya Sutskever, and Mark Chen. GLIDE: towards photorealistic image generation and editing with text-guided diffusion models. In *ICML*, 2022.

Robin Rombach, Andreas Blattmann, Dominik Lorenz, Patrick Esser, and Björn Ommer. High-resolution image synthesis with latent diffusion models. In *Proceedings of the IEEE/CVF Conference on Computer Vision and Pattern Recognition (CVPR)*, pages 10684–10695, June 2022.

Andrew Jaegle, Felix Gimeno, Andrew Brock, Andrew Zisserman, Oriol Vinyals, and João Carreira. Perceiver: General perception with iterative attention. *CoRR*, abs/2103.03206, 2021. URL <https://arxiv.org/abs/2103.03206>.

Chenlin Meng, Yutong He, Yang Song, Jiaming Song, Jiajun Wu, Jun-Yan Zhu, and Stefano Ermon. Sdedit: Guided image synthesis and editing with stochastic differential equations. In *Int. Conf. on Learning Representations (ICLR)*, 2022.

Omri Avrahami, Ohad Fried, and Dani Lischinski. Blended latent diffusion. *CoRR*, abs/2206.02779, 2022.

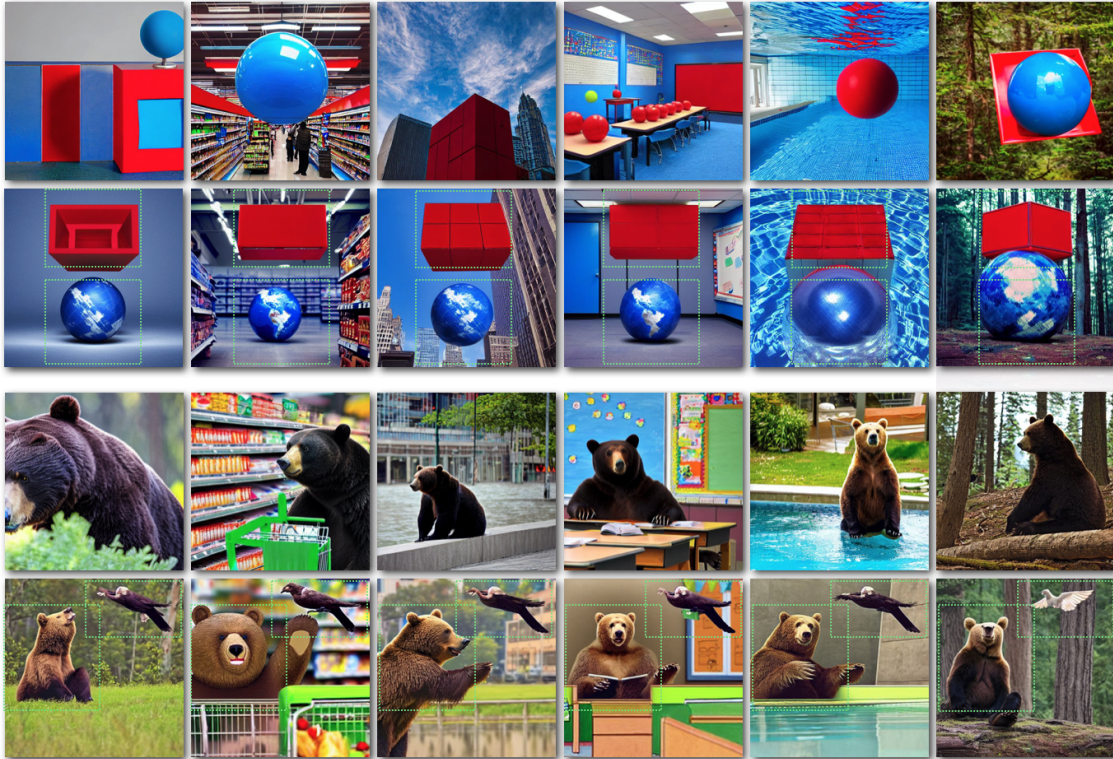


Figure 8: Two directed objects. The second and fourth rows show DD directing two objects with the green bounding boxes. For comparison, the first and third rows show the SD results on the same prompt. The first column is the original prompt “A red cube above the blue sphere” and “A bear watching a bird”, respectively, followed by columns appending various contexts at the end of the prompt: “in the supermarket”, “in the city”, “in the classroom”, “in the swimming pool”, and “in the forest”.

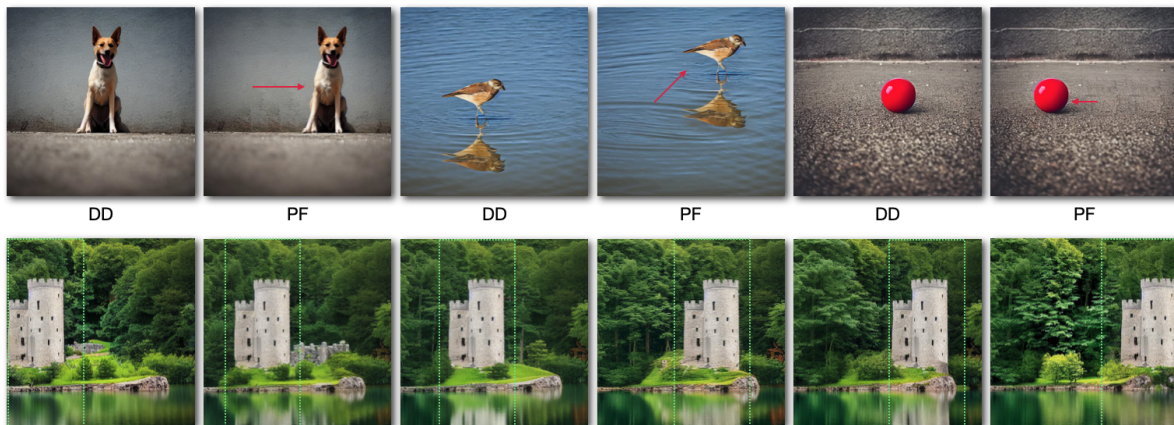


Figure 9: (Top) placement finetuning (PF) allows the position of an object to be changed while largely preserving the object identity and existing background, and without requiring network optimization or fine-tuning. (Bottom) PF is used to explore different locations for a desired castle. Compare to Fig. 7, top, where repositioning the DD bounding box results in a different castle at each location.

Amir Hertz, Ron Mokady, Jay Tenenbaum, Kfir Aberman, Yael Pritch, and Daniel Cohen-Or. Prompt-to-prompt image editing with cross attention control. *arXiv preprint arXiv:2208.01626*, 2022.

Weixi Feng, Xuehai He, Tsu-Jui Fu, Varun Jampani, Arjun R. Akula, Pradyumna Narayana, Sugato Basu, Xin Eric Wang, and William Yang Wang. Training-free structured diffusion guidance for compositional text-to-image synthesis. *CoRR*, abs/2212.05032, 2022.

Binxin Yang, Shuyang Gu, Bo Zhang, Ting Zhang, Xuejin Chen, Xiaoyan Sun, Dong Chen, and Fang Wen. Paint by example: Exemplar-based image editing with diffusion models. *CoRR*, abs/2211.13227, 2022.

- Dani Valevski, Matan Kalman, Yossi Matias, and Yaniv Leviathan. Unitune: Text-driven image editing by fine tuning an image generation model on a single image. *arXiv preprint arXiv:2210.09477*, 2022.
- Bahjat Kawar, Shiran Zada, Oran Lang, Omer Tov, Huiwen Chang, Tali Dekel, Inbar Mosseri, and Michal Irani. Imagic: Text-based real image editing with diffusion models. *arXiv preprint arXiv:2210.09276*, 2022.
- Nan Liu, Shuang Li, Yilun Du, Antonio Torralba, and Joshua B. Tenenbaum. Compositional visual generation with composable diffusion models. In *ECCV*, 2022.
- Dong Huk Park, Grace Luo, Clayton Toste, Samaneh Azadi, Xihui Liu, Maka Karalashvili, Anna Rohrbach, and Trevor Darrell. Shape-guided diffusion with inside-outside attention, 2022. URL <https://arxiv.org/abs/2212.00210>.
- Xichen Pan, Pengda Qin, Yuhong Li, Hui Xue, and Wenhui Chen. Synthesizing Coherent Story with Auto-Regressive Latent Diffusion Models, 2022.
- Jonathan Ho and Tim Salimans. Classifier-free diffusion guidance. In *NeurIPS 2021 Workshop on Deep Generative Models and Downstream Applications*, 2021.
- Adam Paszke, Sam Gross, Soumith Chintala, Gregory Chanan, Edward Yang, Zachary DeVito, Zeming Lin, Alban Desmaison, Luca Antiga, and Adam Lerer. Automatic differentiation in pytorch. 2017.
- Katherine Crowson. k-diffusion. <https://github.com/crowsonkb/k-diffusion>, 2022.
- Tero Karras, Miika Aittala, Timo Aila, and Samuli Laine. Elucidating the design space of diffusion-based generative models. In *Proc. NeurIPS*, 2022.

## A Implementation

Here we discuss our implementation in more detail. DD is implemented with PyTorch Paszke et al. [2017] and the DIFFUSERS library from Huggingface dif [2023]. We use the pretrained stable diffusion model CompViz/stable-diffusion-v1-4 Rombach et al. [2022] for all our experiments. The classification free guidance scale is 7.5. The Linear Multistep Scheduler implemented in diffusers are used for discrete beta schedules based on k-diffusion Crowson [2022], Karras et al. [2022].

The attention editing stage of the DD pipeline (Fig. 4 and Eq. 1 in the main text), and the scene compositing (section 4.2 and Eq. 2 in the main text), both involve a choice of the number of editing steps  $N$ . This choice is informed by the rate of change of the predicted noise between the steps. Fig. 10 illustrates the norm  $\|\nabla_t \mathbf{z}_t\|$  of the gradient of the latent with respect to the time steps.

As can be seen, there is an initial period of  $\approx 10$  time steps labeled as 40 in x-axis in which the norm is rapidly decreasing, indicated by a yellow arrow in the figure. During this period the initial shape of objects are established. This is seen in Fig. 3 in the main text, which visualizes reconstructions from the VAE decoder  $\mathcal{D}(\cdot)$  and the cross-attention maps  $\mathbf{A}^{(i)}, \forall i \in \{1, \dots, |P|\}$  at several time steps during the denoising.

Following this initial period, there is a subsequent stage in which the latents change more slowly as fine details are filled in (visualized with the green arrow). We run the editing operations during the initial “yellow” phase, while conventional SD refinement is used in the “green” phase. For nearly all experiments we empirically selected  $N = 10$  (indicated with the star in the figure) as the time step to switch from editing to refinement.

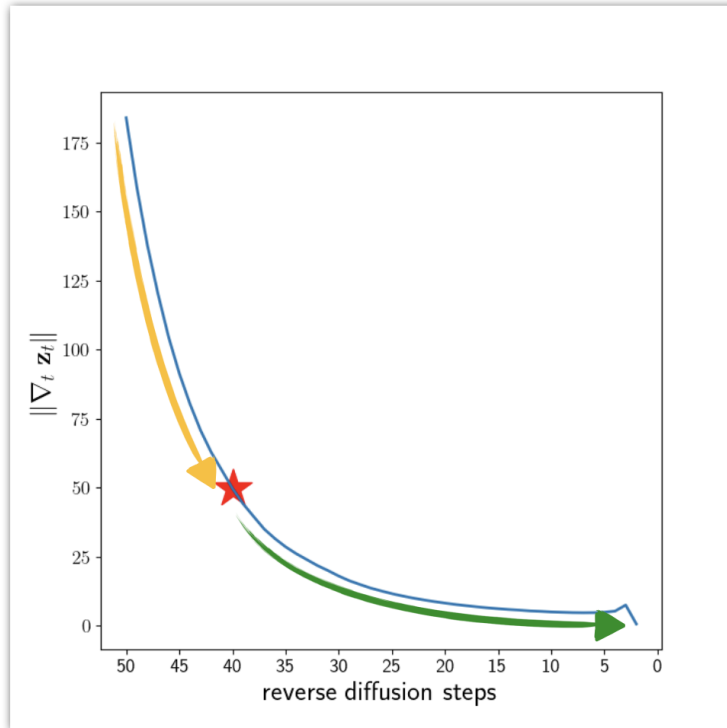


Figure 10: The norm of the gradient of latents with respect to time, plotted across time steps. The yellow and the green arrows indicate two different phases that correspond to our editing and refinement stages.

To optimise Eq. 1 in Sec. 3.2 we use stochastic gradient descent with learning rate 0.05 and momentum 0.99 for 5 iterations of each reverse diffusion step. The vector  $\mathbf{a}$  is initialized with a uniform distribution in the interval  $[0, 1]$  scaled by the constant 0.1. A higher constant tends to lead to an empty background, while very low values fail to guide the directed object.

## B Trailing Attention Maps

A number of text-to-image models use CLIP Radford et al. [2021] embeddings for the text guidance. CLIP accepts an input text representation with up to 77 tokens, including the initial “[CLS]” token representing the sentence level classification. The number of tokens  $|\mathcal{P}|$  in the prompt  $\mathcal{P}$  is generally less than this number. We call the remaining  $\mathcal{T} \in \{k \mid |\mathcal{P}| < k \leq 77 - |\mathcal{P}| - 1\}$  attention maps corresponding to the non-prompt tokens the *trailing attention maps*  $\mathbf{A}^{(i)}, \forall i \in \mathcal{T}$ . Note that the output embedding for [CLS] is not used in our approach.

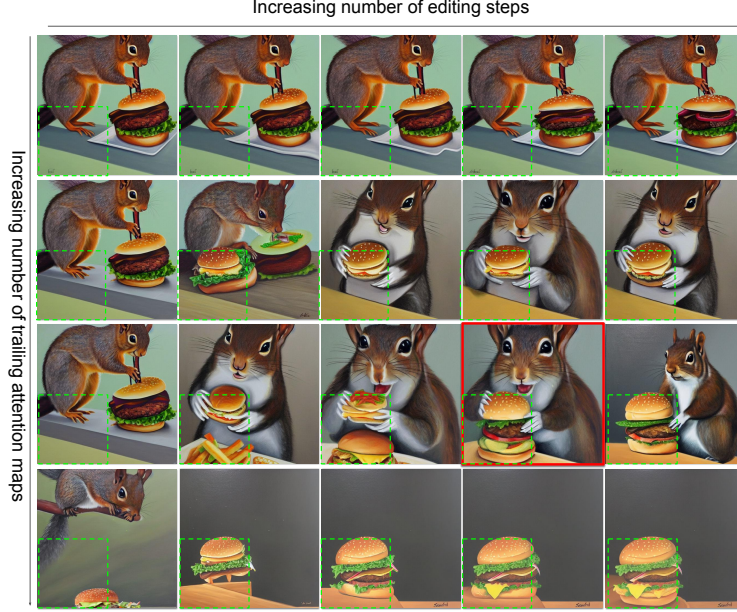


Figure 11: The number of trailing attention maps (5, 10, 15, 20, maps on the vertical axis) versus the number of attention map editing steps (1, 3, 5, 10, and 15 steps on the horizontal axis). The prompt is “A photo of a squirrel eating a burger” with the directed object “burger” positioned at the bottom left. The best results are obtained with an intermediate number of editing steps and edited trailing attention maps, as in the case of the image with the red border.

We edit the trailing maps by injecting Gaussian-falloff activations inside the user-specified bounding box, resulting in the targets  $\mathbf{D}^{(i)}$  in section 3.2 and Algo. 1 in the main text. Fig. 11 shows the effect of injecting activations in a specified number of trailing maps, plotted versus the number of attention editing time steps. In this figure the maps are *used directly in the SD computation* rather than used as targets for optimization in Eq. 1.

When the number of edited trailing attention maps is small (e.g., first row,  $|\mathcal{T}| = 5$ ), the image  $\mathbf{x}_0$  is barely modified. In contrast, when the number of edited trailing attention maps is too large (last row),  $\mathbf{x}_0$  is missing the background and satisfies only the bounding box information. Using an intermediate number of edited trailing attention maps results in the image simultaneously portraying the desired semantic content at the desired location(s).

We initially experimented with implementing DD by manually specifying the number of trailing attention maps, however this required a grid search to get desired results. To avoid this, we instead formulate Eq. 1 to automatically obtain the best combination of the trailing attention maps to control the directed object.

It may not be initially obvious why the trailing attention maps should affect object placement, nor why we would want to use them. While the DIFFUSERS library implements multi-head attention and a variety of conditioning mechanisms, the effect of the trailing maps can be seen from considering a generic cross attention scheme. The cross attention maps  $\mathbf{A}^{(i)} = \text{Softmax}(\mathbf{Q}\mathbf{K}^{(i)T}), \forall i \in \{1, \dots, |\mathcal{W}|\}$  where  $\mathbf{Q} \in \mathbb{R}^{n^2 \times L}$  and  $\mathbf{K} \in \mathbb{R}^{|\mathcal{W}| \times L}$ , are essentially the cross-covariance of each “pixel” of the projected embedding of the SD latent  $z_t$  with projected embeddings of the  $|\mathcal{W}| = 77$  potential words from the prompt. Consider the standard cross-attention computation  $\mathbf{C} = \text{Softmax}(\mathbf{Q}\mathbf{K}^T) \cdot \mathbf{V}$ , where  $\mathbf{V} \in \mathbb{R}^{|\mathcal{W}| \times L}$  is a second projected text embedding of dimension  $L$  for each token. The resulting conditioning matrix  $\mathbf{C}$  has dimension  $\mathbb{R}^{n^2 \times L}$ , while a single “pixel” of this matrix is a convex sum (from the softmax) of all the embeddings in  $\mathbf{V}$ , including those in the trailing words.

Manipulating the trailing maps thus influences the conditioning used in the (classifier-free) text guidance. The optimization scheme in Eq. 1 in the main text uses trailing maps to provide a clean separation between the desired object location (specified via the trailing maps at time step  $t$ ) and the computed attention map at time  $t - 1$ . As stated in the main text, we believe that this intermediate denoising step serves the purpose of moving our position guidance near the range of values expected by the pretrained SD model. The optimization exploits the fact that the maps do not have identical effects (ultimately due to the random initialization of the model), to find a weighted combination that successfully produces the desired object direction.

## C Societal Impact

The aim of this project is to extend the capability of text-to-image models to visual storytelling. In common with most other technologies, there is potential for misuse. In particular, generative models reflect the biases of their training data, and there is a risk that malicious parties can use text-to-image methods to generate misleading images. The authors believe that it is important that these risks be addressed. This might be done by penalizing malicious behavior through the introduction of appropriate laws, or by limiting the capabilities of generative models to serve this behavior.